European Journal of Radiology 117 (2019) 156–163

Contents lists available at ScienceDirect

European Journal of Radiology

journal homepage: www.elsevier.com/locate/ejrad

Research article

Histogram analysis of diffusion kurtosis imaging in the differentiation of malignant from benign breast lesions

Wei Liu[a,1], Chaogang Wei[a,1], Jiayuan Bai[a], Xin Gao[b], Lijuan Zhou[a,*]

[a] Department of Radiology, The Second Affiliated Hospital of Soochow University, Suzhou 215004, China
[b] Department of Radiology, Suzhou Dushuhu Public Hospital (Soochow University Multi-Disciplinary Polyclinic), Suzhou 215004, China

ARTICLE INFO

Keywords:
Diffusion-weighted imaging
Magnetic resonance imaging
Data analysis
Breast lesion
Comparative study

ABSTRACT

Objective: To assess the diagnostic accuracy of histogram analysis of diffusion kurtosis imaging (DKI) in breast lesions.

Materials and methods: Our institutional review board approved this retrospective study. Seventy-two breast lesions (30 benign and 42 malignant) in 71 patients were histopathologically confirmed. All breast lesions were evaluated by 3.0-T diffusion-weighted imaging (DWI) with 4 b-values of 0, 500, 800, and 2000s/mm^2 and dynamic contrast-enhanced magnetic resonance imaging (DCE-MRI). Histogram analyses of conventional DWI and DKI were performed using FireVoxel software for whole lesions. The parameters included apparent diffusion coefficient (ADC), diffusivity (D), and kurtosis (K). The metrics of ADC and DKI parameters (D and K) for benign lesions were compared with those for malignant lesions. The effectiveness of the ADC and DKI parameters (D and K) for diagnosing breast lesions was analysed using receiver operating characteristic (ROC) regression models.

Results: For the malignant breast lesions, the mean, median, and 10th/25th/75th percentile values of ADC and D were significantly lower, while the skewness of ADC and D were significantly higher in comparison of the benign lesions(all $p < 0.05$). The malignant lesions had significantly higher mean, median, and 10th/25th/75th/90th percentile K values than did the benign lesions (all $p < 0.05$). Within each set of parameters, the 10th percentile ADC (Az = 0.752) and D, (Az = 0.834) coupled with the 75th percentile K (Az = 0.904) were the best metrics for differentiating benign from malignant breast lesions. After comparing the parameters in pairs, the Az for the 75th percentile K was significantly higher than that for the 10th percentile ADC ($p = 0.0321$) in differentiating benign from malignant breast lesions. When comparing the combination of the 75th percentile K and the 10th percentile D (Az = 0.937) with the 10th percentile D, 75th percentile K and the mean K, a significantly higher Az was observed for the combination than that for the 10th percentile D and the mean K ($p = 0.0097$ and $p = 0.0431$, respectively). The diagnostic sensitivity and specificity of the combination of the 75th percentile K and the 10th percentile D were 85.71% and 93.33%, respectively.

Conclusion: Histogram analysis of DKI can accurately reflect the histologic characteristics and heterogeneity and is a reliable method for diagnosing breast lesions.

1. Introduction

Breast cancer is one of the most common malignant tumours in women worldwide. Magnetic resonance imaging (MRI) is increasingly used in the clinic as an important imaging method for diagnosing breast lesions. MRI has emerged as a powerful tool in the detection, diagnosis, and staging of breast cancer [1,2]. Dynamic contrast-enhanced magnetic resonance imaging (DCE-MRI) is the most common MRI technique to describe the morphological features and haemodynamic characteristics of breast lesions. DCE-MRI has a high sensitivity but low specificity because of the background parenchymal enhancement and overlap of kinetic enhancement patterns in benign and malignant breast lesions [3–5].

As a functional method of MRI that can reflect the diffusion of water molecules in living tissues, diffusion-weighted imaging (DWI) has been demonstrated to be an effective adjunctive sequence to DCE-MRI [6] and can improve the diagnostic accuracy of MRI in breast cancer. The apparent diffusion coefficient (ADC), which is produced by using a

* Corresponding author at: Lijuan Zhou Department of Radiology, The Second Affiliated Hospital of Soochow University, No. 1055 Sanxiang Road, Gusu District, Suzhou, Jiangsu, 215000, China.
E-mail address: zlj1971sz@126.com (L. Zhou).
[1] The first two authors contributed equally to the work.

https://doi.org/10.1016/j.ejrad.2019.06.008
Received 31 July 2018; Received in revised form 8 May 2019; Accepted 11 June 2019

Table 1
Breast MRI Sequences and Parameters.

Parameter	T_1WI	T_2WI	fat-suppressed T2WI	DWI	fat-suppressed DCE-MRI
Sequence	TSE	TSE	TSE/SPAIR	EPI	THRIVE
Orientation	Axial Bilateral	Axial Bilateral	Axial Bilateral	Axial Bilateral	Axial Bilateral
TR/ TE(ms)	677/8	4502/120	4645/70	5248/77	6.9/3.6
Bandwidth	224.3	335.0	220.6	38.9	949.8
Number of signals acquired	1	1	1	2	1
Matrix	400 × 400	512 × 512	512 × 512	288 × 288	512 × 512
Slice thickness(mm)	3	3	3	5	5
Slice spacing(mm)	0	0	0	0	−2.5
Imaging time (min)	1:05	1:00	1:54	3:56	8:39
B values(s/mm^2)	–	–	–	0,500,800,2000	

Note: THRIVE: T1 high resolution isotropic volume examination.

monoexponential fit, is a quantitative parameter reflecting the diffusion behaviour of water molecules in conventional DWI for b-values less than 1000s/mm^2. Differences in the ADC between benign and malignant breast lesions have been demonstrated in several previous studies [6–11]. However, the ADC thresholds used to identify malignant and benign breast lesions were variable in these studies. The inconsistent ADC thresholds may have been due to the analysis models used. The ADC is based on the assumption that the water diffusion follows a Gaussian pattern, which results in a linear decay of the natural logarithm of the DWI signal intensity as the b-value increases. However, as the b-value increases, the logarithmic signal intensity decay plot no longer maintains a linear shape but, rather, exhibits a distinct curvature with a positive deviation from the plot of the monoexponential model, which indicates that the water diffusion in biological tissues deviates from Gaussian predictions, and thus, other models should be applied. Diffusion kurtosis imaging (DKI), first presented by Jensen et al. in 2005, is an analytical model that describes the diffusive movement of water molecules with a non-Gaussian distribution [12,13]. Previous studies have demonstrated that DKI can well characterize water diffusion in the brain, liver, kidney, bladder and prostate [14–18]. Additionally, several studies used DKI to assess breast lesions and concluded that DKI was more valuable than conventional DWI [19–21].

However, previous studies were limited to using the mean value of DKI parameters based on a region of interest (ROI) from a single representative slice of a lesion or a smaller ROI in the highest signal region [19–21], which does not fully reflect the various biological heterogeneities of the whole tumour. Histogram analysis of the whole breast lesion may offer multiple parameters to determine the distribution of quantitative parameters, including percentiles, minimal and maximal values, kurtosis, and skewness, thus providing more information about the tumour heterogeneity than the mean values. Therefore, histogram analysis may be used to better differentiate benign or malignant tumours and guide clinical treatment.

This study aims to investigate the diagnostic efficiency of the histogram analysis of DKI parameters of the whole benign or malignant breast lesion and to determine which DKI and ADC parameters can best differentiate malignant from benign breast lesions using 3.0 T MRI.

2. Materials and methods

2.1. Patients

This retrospective study was approved by our institutional review board, and the requirement for informed consent was waived. Between October 2015 and May 2017, 198 women were pathologically diagnosed with breast lesions by core-needle biopsy or tumour resection within two weeks after MRI. The following patients were excluded: patients who had undergone prior neoadjuvant chemotherapy before MRI, patients who had undergone core-needle biopsy before MRI, patients who had poor diffusion-weighted image quality, and patients with lesions less than 1 cm in size. Therefore, a total of 71 female patients (median age: 41 years; range: 13–64 years) with 72 lesions were included in this study. One patient had two benign lesions. Forty-two (58.3%) lesions were diagnosed as malignant, and 30 (41.7%) lesions as benign. The malignant lesions included 5 intraductal carcinomas in situ, 35 invasive ductal carcinomas, 1 invasive lobular carcinoma, and 1 mucinous cancer. The benign lesions included 19 fibroadenomas, 6 granulomatous lesions, 1 benign phyllodes tumors, and 4 intraductal papillomas.

2.2. MRI technique

Bilateral breast MRI examination was performed for all patients with a 3.0 T MRI scanner (Ingenia, Philips Medical Systems, the Netherlands) and a dedicated sixteen-channel bilateral breast surface coil. T_2-weighted, fat-suppressed T_2-weighted, T_1-weighted, DW and DCE-MR images in the axial plane were obtained. DWI was performed using single-shot spin-echo planar imaging (EPI) with 4 b-values of 0, 500, 800 and 2000s/mm^2 in the x, y and z directions. DCE-MRI was performed with a fat-suppressed T_1 sequence before and after injection of gadolinium chelate at a dose of 0.1 mmol/kg and a rate of 2.0 mL/s, followed by flushing with 20 mL saline solution. We included 35 dynamics of the DCE imaging, and the total scan time of the DCE-MRI lasted 8.39 min, with each dynamic scan lasting 14.8 s. The MRI sequences and parameters are shown in Table 1.

2.3. Image analysis

Breast MR images were reviewed by two independent breast radiologists with 9 years and 20 years of experience in breast MRI, who had no warning of the specific pathological diagnosis results. Lesion features were recorded according to the American College of Radiology Breast Imaging Reporting and Data System (ACR BI-RADS) MRI lexicon [22].

DW images were first analysed voxel-by-voxel using a monoexponential decay model with b = 0 and 800 s/mm^2 to produce ADC maps. Kurtosis maps and diffusivity maps were produced from diffusion kurtosis (DK) models with b-values of 0, 500, 800, and 2000 by using an in-house software (FireVoxel; MATLAB). For the DK models, we analysed non-Gaussian water diffusivity by using the following equation: $S(b) = S0e(-bD + 1/6b^2D^2K)$, where S(b) is the DWI signal at a particular b-value, S0 is the baseline signal without diffusion weighting, D is the apparent diffusion parameter for a non-Gaussian distribution, and K is the apparent kurtosis coefficient. The edges of the lesions of interest were located according to DWI and DCE-MRI. ROIs including the whole tumour were manually drawn slice by slice on DW images with a b-value of 800 s/mm^2, avoiding necrosis, cystic changes, and large vessel areas, and then copied onto the ADC, D and K maps. ROIs were drawn

by two independent breast radiologists. Voxel analysis of each tumour was performed, and the corresponding data were calculated using SPSS software (version 20.0) for histogram analysis. The cumulative D, K and ADC for the whole lesion were obtained from respective histogram analyses. In this study, the histogram-derived parameters of D, K and ADC were recorded as the mean, median, 10th, 25th, 75th, and 90th percentiles (the *n*th percentile indicates the point at which *n*% of the voxel values from the histogram are located to the left), skewness (measure of asymmetry of a distribution), and kurtosis (measure of the sharpness of the peak of a distribution).

3. Statistical analysis

SPSS (version 20.0) and MedCalc (version 15.0) were used for statistical analyses. Interobserver reliability for the ADC, D and K histogram parameter measurements of the two researchers was assessed by using the interclass correlation coefficient (ICC). The ICC was explained as follows: poor agreement, 0.00 to 0.20; fair agreement, 0.21 to 0.40; moderate agreement, 0.41 to 0.60; good agreement, 0.61 to 0.80; excellent agreement, 0.81-1.00. The Kolmogorov-Smirnov test was used to check whether the measurement data followed a normal distribution, and the data following a normal distribution were indicated as median values. The differences in D, K and ADC parameters between benign and malignant lesions were tested with independent-sample *t* tests. The differences in skewness and kurtosis were tested with the Mann-Whitney U test. The efficiency of D, K and ADC parameters in the diagnosis of benign and malignant breast lesions was analysed using a receiver operating characteristic (ROC) regression model and quantified using the area under the ROC curves (*Az*). Comparisons between the *Az* for histogram-derived parameters were performed with the method described by DeLong et al. [23]. The diagnostic efficacies, including sensitivity, specificity and Youden index, were generated based on the cut-off point. $p < 0.05$ was considered statistically significant.

4. Results

4.1. Interobserver agreement

ICCs for measurements of ADC, D and K histogram parameters which were calculated to assess the stability of parameters obtained by the two observers are summarized in Table 2. Overall, the interobserver agreement is excellent for the histogram-derived values including the mean, median, $10^{th}/25^{th}/75^{th}/90^{th}$ percentiles ADC, D and K (ICC range, 0.847–0.984), and good for the histogram-derived values of the skewness and kurtosis of the all three parameters (ICC range, 0.695–0.774).

Table 3
Histogram parameters of ADC, D and K in benign and malignant breast lesions.

Variable	Benign(n = 30)	Malignant(n = 42)	P value
Histogram ADC ($\times 10^{-3}$ mm²/s)			
Mean	1.34(1.13, 1.59)	1.10(0.99, 1.30)	0.005
10th Percentile	1.09(0.93, 1.24)	0.79(0.69, 0.92)	0.001
25th Percentile	1.26(1.04, 1.41)	0.94(0.84, 1.08)	0.001
Median	1.34(1.12, 1.60)	1.08(0.95, 1.26)	0.004
75th Percentile	1.50(1.22, 1.75)	1.22(1.09, 1.50)	0.016
90th Percentile	1.64(1.39, 1.94)	1.39(1.24, 1.67)	0.058
Skewness[a]	0.08(-0.37, 0.41)	0.43(-0.01, 0.76)	0.009
Kurtosis[a]	0.48(-0.16, 1.11)	0.38(-0.13, 1.17)	0.683
Histogram D ($\times 10^{-3}$ mm²/s)			
Mean	1.58(1.35, 1.89)	1.32(1.18, 1.45)	0.000
10th Percentile	1.26(1.03, 1.47)	0.85(0.76, 1.05)	0.000
25th Percentile	1.44(1.18, 1.70)	1.09(0.99, 1/17)	0.000
Median	1.60(1.34, 1.88)	1.31(1.14, 1.41)	0.000
75th Percentile	1.77(1.62, 2.06)	1.50(1.37, 1.73)	0.003
90th Percentile	1.98(1.71, 2.21)	1.74(1.53, 2.11)	0.059
Skewness[a]	0.04(-0.45, 0.40)	0.40(0.01, 0.69)	0.020
Kurtosis[a]	0.40(-0.23, 0.75)	0.31(-0.20, 1.28)	0.368
Histogram K			
Mean	0.72(0.55, 0.80)	0.99(0.87, 1.04)	0.000
10th Percentile	0.49(0.33, 0.62)	0.74(0.59, 0.80)	0.000
25th Percentile	0.60(0.47, 0.69)	0.84(0.75, 0.90)	0.000
Median	0.69(0.55, 0.79)	0.97(0.88, 1.03)	0.000
75th Percentile	0.75(0.63, 0.92)	1.10(1.04, 1.22)	0.000
90th Percentile	0.80(0.68, 1.03)	1.25(1.15, 1.33)	0.000
Skewness[a]	−0.11(-0.90, 0.51)	0.04(-0.62, 0.74)	0.392
Kurtosis[a]	1.85(0.10, 4.53)	0.85(0.25, 2.72)	0.416

Note: Unless otherwise specified, Data was median values. Numbers in parentheses were interquartile ranges. Date was analyzed by independent-sample *t* test.

[a] Data analyzed by Mann-Whitney *U* test.

4.2. Comparison of histogram-derived ADC, D and K values between benign and malignant breast lesions

The median (interquartile range (IQR)) of all histogram-derived parameters for both benign and malignant breast lesions is shown in Table 3. Two representative cases from each group are shown in Figs. 1 and 2, respectively. Boxplots of the 10th percentile ADC, 10th percentile D and 75th percentile K are shown in Fig. 3. For ADC and D, the histogram-derived values including the mean, median, 10th/25th/75th percentiles for malignant lesions were significantly lower than those for benign lesions (all $p < 0.05$), but the skewness for malignant lesions was significantly higher than that for benign lesions ($p < 0.05$). No significant difference was found in the 90th percentile or kurtosis between benign and malignant lesions (all $p > 0.05$). Furthermore, the malignant lesions had significantly higher K values than the benign

Table 2
ICC* for measurements of ADC, D and K histogram parameters.

ADC	Mean	10^{th}	25^{th}	Median	75^{th}	90^{th}	Skewness	Kurtosis
ICC	0.984 (0.974-0.990)	0.913 (0.861-0.945)	0.924 (0.879-0.953)	0.980 (0.968-0.987)	0.976 (0.962-0.985)	0.945 (0.912-0.965)	0.772 (0.635-0.857)	0.736 (0.579-0.835)
D	Mean	10^{th}	25^{th}	Median	75^{th}	90^{th}	Skewness	Kurtosis
ICC	0.930 (0.888-0.956)	0.946 (0.913-0.966)	0.926 (0.882-0.954)	0.933 (0.893-0.958)	0.871 (0.793-0.919)	0.862 (0.780-0.914)	0.774 (0.638-0.858)	0.695 (0.512-0.809)
K	Mean	10^{th}	25^{th}	Median	75^{th}	90^{th}	Skewness	Kurtosis
ICC	0.940 (0.904-0.963)	0.847 (0.756-0.904)	0.925 (0.881-0.953)	0.939 (0.902-0.962)	0.941 (0.906-0.963)	0.893 (0.829-0.933)	0.773 (0.637-0.858)	0.711 (0.538-0.819)

Note: *ICC = Interclass correlation coefficient. Numbers in parentheses are 95% confidence intervals.

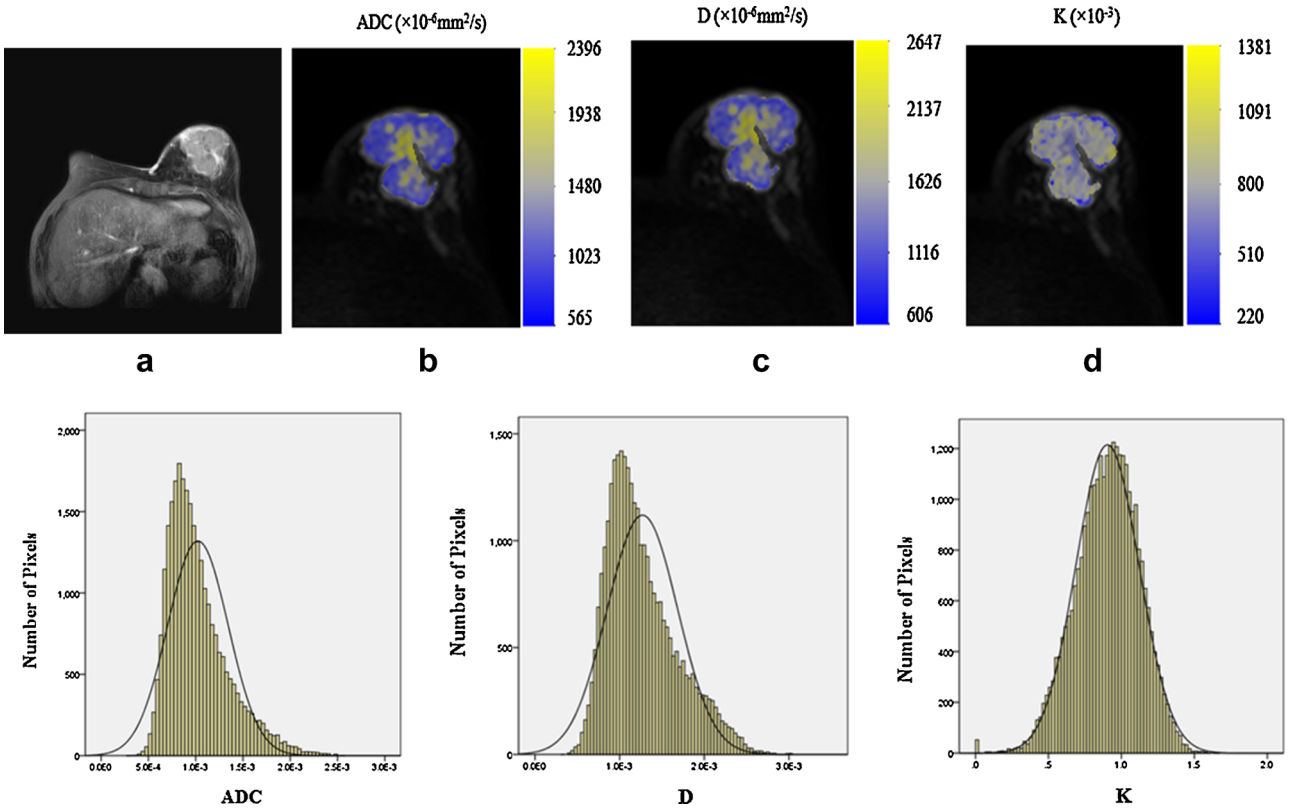

Fig. 1. A 64-year-old woman with invasive ductal carcinoma in her left breast. (a) Dynamic enhanced image, (b) Corresponding ADC image delineated through hand-drawn ROI, (c) Corresponding D image of the lesion, (d) Corresponding K image. Histogram of the lesion showed a lower ADC, D values and lager K values relatively.

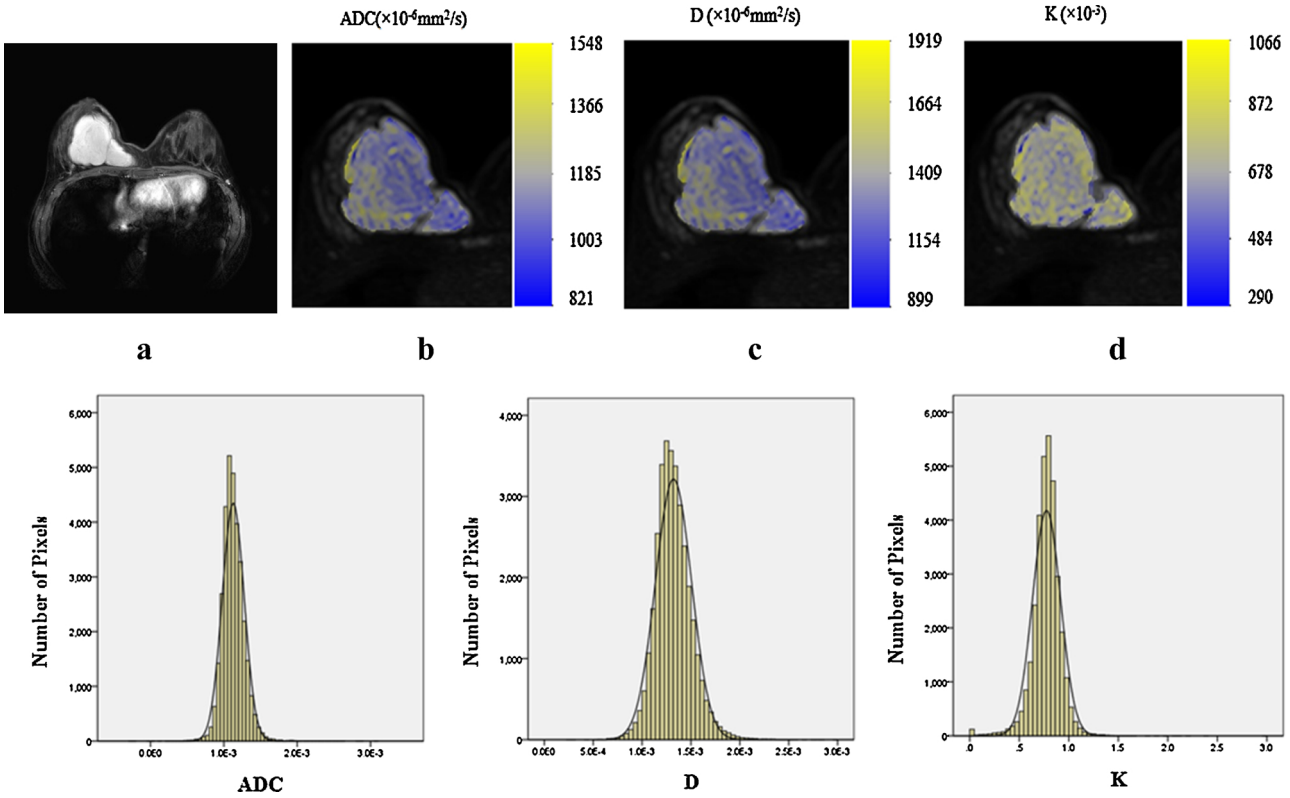

Fig. 2. A 21-year-old girl with a giant fibroadenoma in her right breast. (a) Dynamic enhanced image, (b) Corresponding ADC image delineated through hand-drawn ROI, (c) Corresponding D image of the lesion, (d) Corresponding K image. Histogram of the whole lesion showed lager ADC, D values and lower K values relatively.

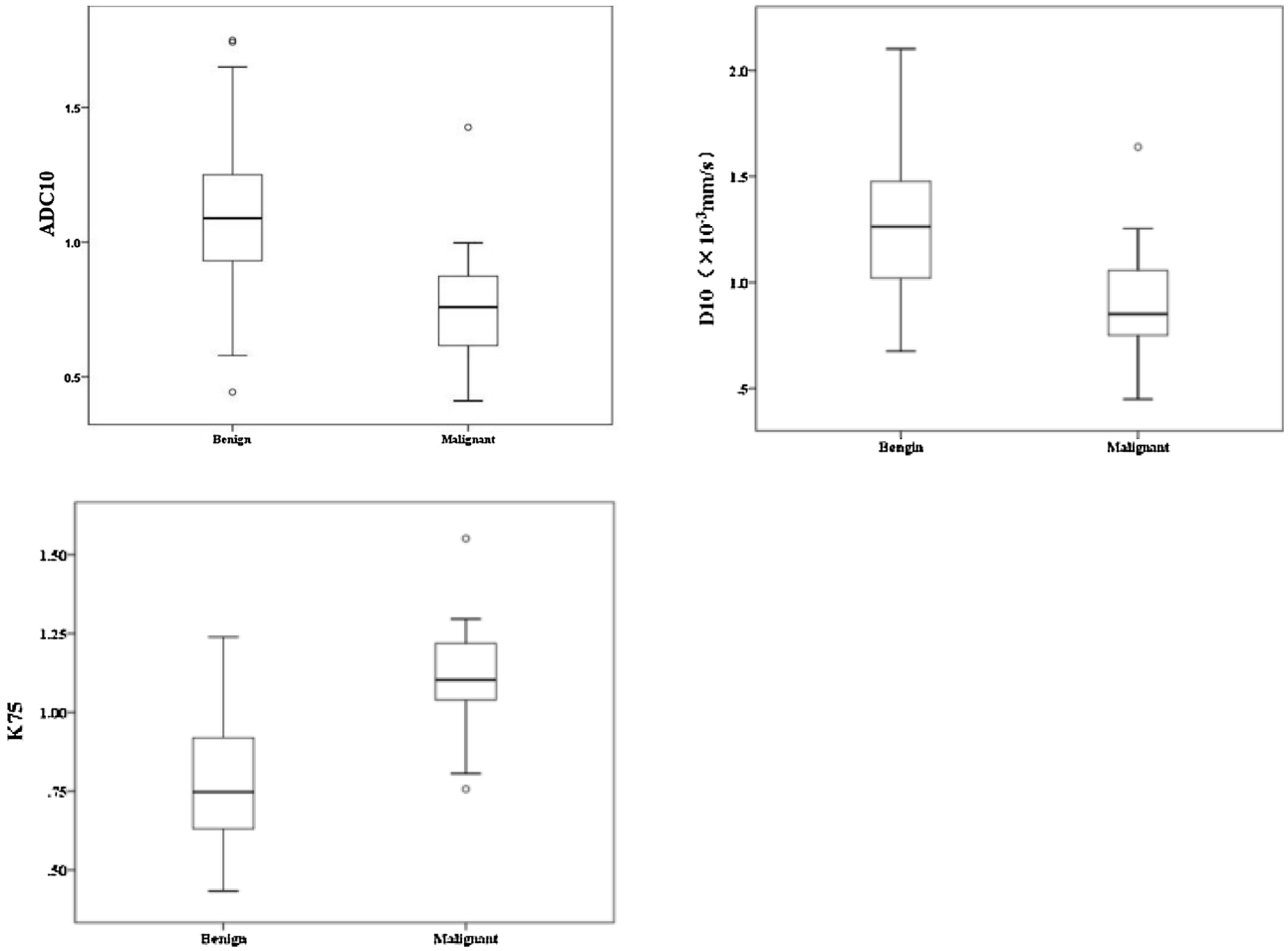

Fig. 3. Boxplots show ADC10, D10, and K75 in benign and malignant lesions.

lesions in the histogram-derived mean, median, 10^{th}/25^{th}/75^{th} and 90^{th} percentiles (all $p < 0.05$). However, no significant difference was observed in the skewness or kurtosis of K between benign and malignant lesions (all $p > 0.05$).

4.3. Diagnostic performance of histogram-derived ADC, D and K values for benign and malignant breast lesions

The results of the ROC analysis to assess the diagnostic efficacy for distinguishing benign from malignant lesions are summarized in Tables 4 and 5 and Fig. 4. Within each set of parameters, the 10th percentile ADC and D, coupled with the 75th percentile K had the highest *Az* values. When compared with their respective mean values, the 10^{th} and 25^{th} percentile ADC, the 10^{th} percentile D had significantly higher *Az* values. The 75^{th} percentile K also had a higher *Az* than did the mean K, albeit without a significant difference. Comparing the *Az* of the mean ADC, mean D and mean K revealed that the mean K had a significantly higher *Az* than that of the mean ADC ($z = 2.409$, $p = 0.0160$).

As shown in Fig. 4d, we compared the best ADC, D and K histogram-derived parameters (the 10^{th} percentile ADC, 10^{th} percentile D, and 75^{th} percentile K). The 75^{th} percentile K showed the highest *Az* ($Az = 0.904$) among the best three parameters, and compared to the 10^{th} percentile ADC, this advantage was statistically significant ($z = 2.143$, $p = 0.0321$). Moreover, the *Az* ($Az = 0.937$) for the combination of the 75^{th} percentile K and the 10^{th} percentile D which were derived from the same DKI model was significantly higher than that for the 10^{th} percentile D and mean K ($z = 2.587$, $p = 0.0097$; $z = 2.023$, $p = 0.0431$). The *Az* for the combination of the 75^{th} percentile K and the 10^{th} percentile D was also higher than that for the 75^{th} percentile K, although

Table 4
Diagnosis efficiency of histogram parameters of ADC, D and K for benign and malignant breast lesions.

Variable *Az*		Sensitivity	Specificity	Youden index	95%CI
Histogram ADC					
Mean	0.690	73.81	70.00	0.4381	0.570-0.794
10th[a] Percentile	0.752	78.57	76.67	0.5524	0.637-0.847
25th Percentile	0.729	73.81	73.33	0.4714	0.612-0.827
Median	0.697	73.81	70.00	0.4381	0.577-0.800
75th Percentile	0.671	69.05	66.67	0.3571	0.550-0.777
Skewness	0.674	50.00	80.00	0.3000	0.553-0.780
Histogram D					
Mean	0.749	83.33	70.00	0.5333	0.633-0.844
10th[a] Percentile	0.834	71.43	86.67	0.5810	0.728-0.911
25th Percentile	0.800	80.95	73.33	0.5429	0.689-0.885
Median	0.763	83.33	70.00	0.5333	0.649-0.856
75th Percentile	0.694	66.67	73.33	0.4000	0.575-0.798
Skewness	0.683	64.29	66.67	0.3095	0.562-0.787
Histogram K					
Mean	0.875	83.33	83.33	0.6667	0.775-0.941
10th Percentile	0.784	69.05	83.33	0.5238	0.671-0.872
25th Percentile	0.832	76.19	86.67	0.6286	0.725-0.910
Median	0.894	90.48	83.33	0.7381	0.799-0.954
75th[a] Percentile	0.904	85.71	93.33	0.7905	0.811-0.961
90th Percentile	0.863	83.33	86.67	0.7000	0.762-0.933
75th K + 10th D	0.937	85.71	93.33	0.7905	0.854-0.981

Note: Date was percentage.
[a] With the highest values in *Az*.

Table 5
Comparison of Az of ADC, D and K histogram parameters of differentiating breast lesions.

ADC	Mean	10th	25th	Median	75th	Skewness
Az	0.690 (0.570-0.794)	0.752 (0.636-0.846)	0.729 (0.612-0.827)	0.697 (0.577-0.800)	0.671 (0.550-0.777)	0.674 (0.554-0.780)
Z value	Ref	2.316	2.531	0.996	1.144	0.203
P value	Ref	0.0206	0.0114	0.3194	0.2526	0.8393
D	Mean	10th	25th	Median	75th	Skewness
Az	0.749 (0.633-0.844)	0.834 (0.728-0.911)	0.800 (0.689-0.885)	0.763 (0.649-0.856)	0.694 (0.575-0.798)	0.683 (0.562-0.787)
Z value	Ref	2.109	1.634	1.536	2.890	0.842
P value	Ref	0.0350	0.1022	0.1245	0.0038	0.4000
K	Mean	10th	25th	Median	75th	90th
Az	0.875 (0.775-0.941)	0.784 (0.671-0.872)	0.832 (0.725-0.910)	0.894 (0.799-0.954)	0.904 (0.811-0.961)	0.863 (0.762-0.933)
Z value	Ref	2.097	1.441	1.155	1.816	0.316
P value	Ref	0.0360	0.1495	0.2480	0.0693	0.7519

Note: Numbers in parentheses were 95% confidence intervals. Ref = reference value.

this difference was not statistically significant (z = 1.262, p = 0.2070). The diagnostic sensitivity and specificity of the combination of the 75th percentile K and the 10th percentile D were 85.71% and 93.33%, respectively.

5. Discussion

The diagnosis and classification of breast lesions using mammography and ultrasound have always been a major challenge, especially for close fibroglandular breasts [24]. As a new non-invasive functional imaging technique for breast examination, MRI has been increasingly used in clinical practice. DCE-MRI is the most common MRI technique in differential diagnosis of breast lesions. DWI has been shown to be an effective adjunctive sequence to DCE-MRI [6].

DWI is a common MRI technique to describe the extent and direction of water diffusion in a tissue. Standard DWI requires acquisition of only two b-values for the calculation of ADC. In clinical body imaging, DWI is typically practised by using b-value up to 800–1000 s/mm^2 and then a monoexponential that assumes Gaussian diffusion is used for quantification [25]. Nevertheless, DWI often reveals the presence of non-Gaussian diffusion at ultrahigh b-value. At this point, the DK model is used to provide more potential information on tissues than that provided by standard monoexponential analysis for b-values greater than 1000s/mm^2. DKI requires the acquisition of at least three diverse b-values including at least two b-values both above and below 1000s/mm^{2}on account of an additional unknown variable (K) within the formula and to facilitate the successful capture of the non- Gaussian behavior. In fact, it makes sense to avoid using too many b-values because of the imaging time [13]. In our study, we used b-value of 0 and 800 s/mm^{2}to produce ADC maps, and 4 b-values of 0, 500, 800 and 2000s/mm^{2}to perform DK model analysis. It is also important for DKI to choose the maximal b-value. When the maximal b-value is not enough, we cannot capture the deviation of the curvature of the signal intensity (SI) decay plot away from Gaussian and the ability of the sequence to measure non-Gaussian diffusion behaviour declines dramatically [26].

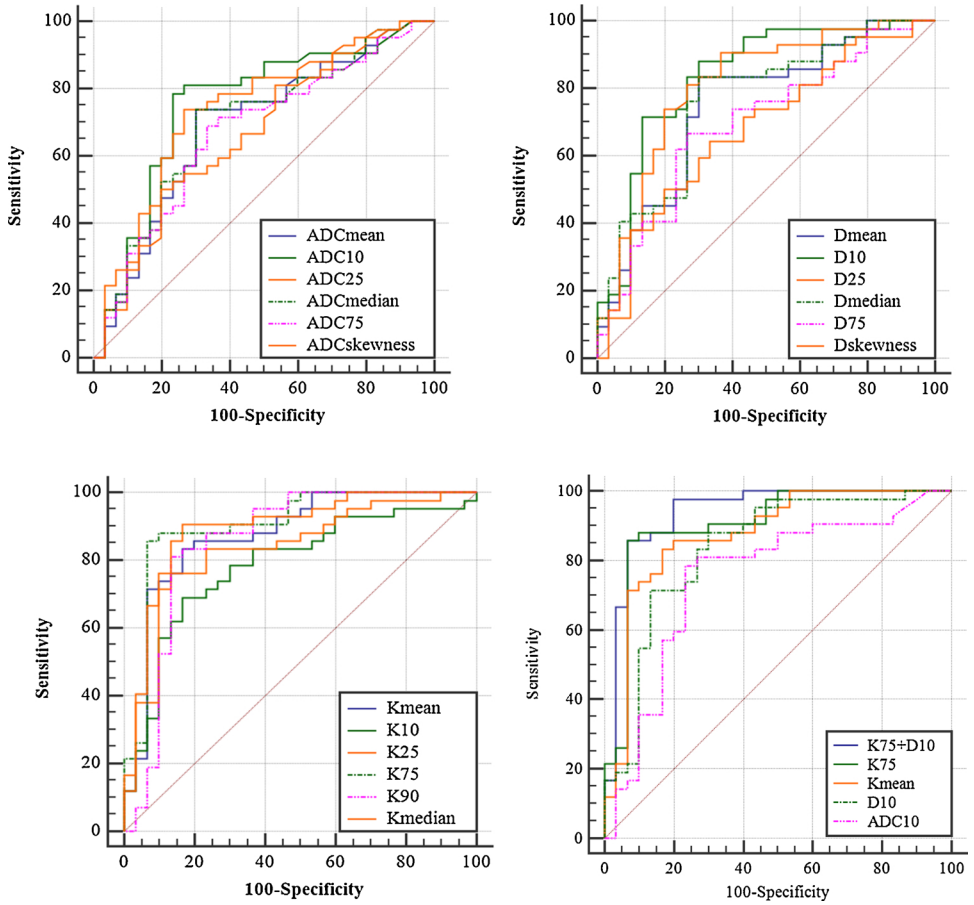

Fig. 4. Comparison of ROC of histogram parameters of ADC, D and K, the 10th ADC, the 10th D and the 75th K have the largest Az for differentiating malignant from benign lesions in their individual histogram parameter group. The 75th K with the 10th D has the largest *Az* among all histogram parameters.

However, if high b-value exceeds 3000 s/mm^2, the measurement of SI will violate assumptions of the DK model so it is discouraged [12,13,27–29]. Most scholars used a maximal b-value of 1500–2000 s/mm^2 in body DKI, and could successfully capture non-Gaussian behaviour of the SI decay plot [13,17,30]. Simultaneously, in order to maintain sufficient signal to noise ratio (SNR), the ultrahigh b-value cannot be too high. So, in our study, we take the b-value with a maximum value of 2000s/mm^{2}for breast DKI and also double the signals acquired for the better SNR of the ultrahigh b-value DWI.

Previous studies were limited in using the mean or median values of DKI parameters based on an ROI from a single representative slice, which may dilute or even mask small but important differences between different disease entities. Additionally, these parameters may not accurately describe the intrinsic characteristics and heterogeneity of the entire lesion. This study is the first work to investigate the performance of whole-lesion histogram analysis, including all voxels from the entire lesion, which reflect the heterogeneity of the lesions.

The mean values of ADC, D and K have been investigated in previous studies [19,22,31]. These studies showed that malignant breast lesions had lower mean ADC and D and higher mean K values than benign breast lesions. Our results were consistent with those of the above studies, indicating that the microstructure of malignant tumours is more complicated than that of benign lesions and that the movement of water molecules in malignant tumours is more restricted than that in benign lesions. In addition, previous research [19,30,31] has shown that the mean K has a greater diagnostic efficacy than the mean ADC. We obtained similar results ($z = 2.409$, $p = 0.0160$). This finding showed that the DK model was more accurate than the conventional ADC for diagnosing breast lesions. The conventional ADC is based on the assumption that water diffusion follows a Gaussian distribution. In fact, in tissues, the destruction of the microenvironment, cellularity, and cell membrane integrity prevent water molecules from spreading and lead to a non-Gaussian distribution. The DK model can describe water diffusion as a non-Gaussian distribution, and it may reflect physiologic and morphologic changes associated with breast lesions more precisely than the conventional DWI. Usually, malignant lesions have more complex and heterogeneous microstructures than benign lesions, which is the basis of distinguishing malignant lesions from benign lesions for K value.

In our study, the 10th percentile ADC and the 10th percentile D, coupled with the 75th percentile K yielded the highest *Az* among their respective groups for differentiating benign from malignant breast lesions. The results were consistent with those of previous studies analysing histogram-derived ADC and DK values [18,30,31]. Liu et al. [30] also found that the 10th percentile ADC demonstrated the best performance in differentiating benign from malignant tumours among all histogram-derived values of the conventional ADC. Suo et al. [31] found that the minimum ADC demonstrated the best accuracy in the identification of breast lesions. We did not use minimum and maximum values because the minimum and maximum ADC values might be more susceptible to outliers resulting from noise, handling, and adjacent structures. Wang et al [18] found that the 10th percentile D and 90th percentile K have relatively higher Az in the DKI model in differentiating low-grade of prostate cancer (LG-PCa) from high-grade of prostate cancer (HG-PCa). These results may be due to the heterogeneity of the tissue lesion. The lower percentiles of ADC and D coupled with the higher percentiles of K can better capture the nature of the most aggressive components in the lesion, which are densely packed with malignant cells. These results indicated that histogram analysis could accurately reflect the histologic characteristics and heterogeneity of breast lesions and could provide more parameters other than the mean values to distinguish malignant breast lesions from benign lesions, and some of those histogram-derived parameters may be more useful than the mean values.

Furthermore, among the three best parameters (the 10th percentile ADC, the 10th percentile D and the 75th percentile K), the 75th percentile K had the highest *Az*. The *Az* for the 75th percentile K was significantly different from that for the 10th percentile ADC. These findings were consistent with previous findings about prostate DKI study which demonstrated that the 90th percentile K had substantial advantage against the 10th ADC for dominantly higher Az [18]. The results indicated that the malignant breast lesions had more complicated and heterogeneous microstructures than the benign lesions, and the difference of the distribution of this complexity and heterogeneity between the malignant lesions and the benign lesions might be more prominent than that of the cellularity, so it might be more useful in the differential diagnosis of the breast lesions. Additionally, our study indicated that the combination of the 75th percentile K and the 10th percentile D which were derived from the same DKI model could improve the diagnostic efficiency, and was superior to any of the parameters alone, this made the histogram analysis of DKI have more dominance in differential diagnosis of the malignant and benign breast lesions than the histogram analysis of the conventional DWI which had only one set of parameters. The results indicated that the DKI parameters may reflect physiologic and morphologic changes associated with breast lesions more precisely than the conventional DWI. DKI might add valuable indications of microstructural changes to conventional DWI for the identification of breast lesions. In turn, it demonstrated that the DWI signal decay in breast tumors does not follow a simple monoexponential mode, and it was necessary to use DK mode to describe the diffusive movement of water molecules with a non-Gaussian distribution.

Our study has several limitations. First, it was a retrospective study, the sample size was small, and there were only a few types of breast lesions. The majority of benign lesions were fibroadenomas, and the majority of malignant lesions were invasive ductal carcinomas, with few cases of other types of breast lesions. All breast lesions included in the study were more than 1 cm in size. All of these factors may have led to a sample selection bias. Second, all parameters in this study were calculated by manually drawing the ROIs, which may have resulted in an inconsistent ROI between parameters. Our study is the first work to investigate the performance of the histogram parameters derived from DK model in diagnosing breast lesions, and it still needs a larger sample size and in-depth study in the future.

6. Conclusion

Our study indicated that the whole-lesion histogram analysis of DK models could accurately reflect the histologic characteristics and heterogeneity of breast lesions, and the multiple parameters of DKI demonstrated a higher diagnostic efficiency than the respective mean values. The 10th percentile ADC, the 10th percentile D and the 75th percentile K demonstrated the highest diagnostic efficiency in their respective groups. Furthermore, among all histogram-derived DKI and ADC parameters, the 75th percentile K was the best metric for differentiating malignant from benign breast lesions. The combination of the 75th percentile K and the 10th percentile D could improve the diagnostic efficiency. Hence, histogram analysis of DKI was more accurate and effective than histogram analysis of ADC. Therefore, histogram analysis of DKI is a reliable method for diagnosing breast lesions.

Acknowledgement

This project is subjected to the second affiliated hospital of Soochow university preponderant clinic discipline group project funding (XKQ2015008).

References

[1] C.D. Lehman, C. Gatsonis, C.K. Kuhl, et al., MRI evaluation of the contralateral breast in women with recently diagnosed breast cancer, N. Engl. J. Med. 356 (2007) 1295–1300.

[2] M. Morrow, J. Waters, E. Morris, MRI for breast cancer screening, diagnosis, and treatment, Lancet 378 (2011) 1804–1811.
[3] W.A. Berg, L. Gutierrez, M.S. NessAiver, et al., Diagnostic accuracy of mammography, clinical examination, US, and MR imaging in preoperative assessment of breast cancer, Radiology 233 (2004) 830–849.
[4] N.H. Peters, I.H. Borel Rinkes, N.P. Zuithoff, et al., Meta-analysis of MR imaging in the diagnosis of breast lesions, Radiology 246 (2008) 116–124.
[5] C. Boetes, S.P. Strijk, R. Holland, et al., False-negative MR imaging of malignant breast tumors, Eur. Radiol. 7 (1997) 1231–1234.
[6] R.H. Ei Khouli, M.A. Jacobs, S.D. Mezban, et al., Diffusion-weighted imaging improves the diagnostic accuracy of conventional 3.0T breast MR imaging, Radiology 256 (2010) 64–73.
[7] W. Bogner, S. Gruber, K. Pinker, et al., Diffusion-weighted MR for differentiation of breast lesions at 3.0T: how does selection of diffusion protocols diagnosis? Radiology 253 (2009) 341–351.
[8] Y. Guo, Y.Q. Cai, Z.L. Cai, et al., Differentiation of clinically benign and malignant breast lesions using diffusion-weighted imaging, J. Magn. Reson. Imaging 16 (2002) 172–178.
[9] C. Marini, C. lacconi, M. Giannelli, et al., Quantitative diffusion-weighted MR imaging in the differential diagnosis of breast lesion, Eur. Radiol. 17 (2007) 2646–2655.
[10] G.G. Lo, V. Ai, J.K. Chan, et al., Diffusion-weighted magnetic resonance imaging of breast lesions: first experiences at 3T, J. Comput. Assist. Tomogr. 33 (2009) 63–69.
[11] Z. Ouyang, Y. Ouyang, M. Zhu, et al., Diffusion-weighted imaging with fat suppression using short-tau inversion recovery: clinical utility for diagnosis of breast lesions, Clin. Radiol. 69 (2014) e337–344.
[12] J.H. Jensen, J.A. Helpern, A. Ramani, et al., Diffusional kurtosis imaging: the quantification of non-gaussian water diffusion by means of magnetic resonance imaging, Magn. Reson. Med. 53 (2005) 1432–1440.
[13] J.H. Jensen, J.A. Helpern, MRI quantification of non-Gaussian water diffusion by kurtosis analysis, NMR Biomed. 2010 (23) (2010) 698–710.
[14] S. Van Cauter, J. Veraart, J. Sijbers, et al., Gliomas: diffusion kurtosis MR imaging in grading, Radiology 263 (2012) 492–501.
[15] S.W. Anderson, B. Barry, J. Soto, et al., Characterizing non-gaussian, high b-value diffusion in liver fibrosis: stretched exponential and diffusional kurtosis modeling, J. Magn. Reson. Imaging 39 (2014) 827–834.
[16] G. Pentang, R.S. Lanzman, P. Heusch, et al., Diffusion kurtosis imaging of the human kidney: a feasibility study, Magn. Reson. Imging 23 (2014) 413–420.
[17] S. Suo, X. Chen, X. Ji, et al., Investigation of the non-Gaussian water diffusion properties in bladder cancer using diffusion kurtosis imaging: a preliminary study, J. Comput. Assist. Tomogr. 39 (2015) 281–285.
[18] Q. Wang, H. Li, X. Yan, et al., Histogram analysis of diffusion kurtosis magnetic resonance imaging in differentiation of pathologic Gleason grade of prostate cancer, Urol. Oncol. 33 (337) (2015) Elsevier, e15-337.e24.
[19] K. Sun, X. Chen, W. Chai, et al., Breast cancer: diffusion kurtosis MR imaging-diagnostic accuracy and correlation with clinical pathologic factors, Radiology 277 (2015) 46–55.
[20] L. Nogueira, S. Brandao, E. Matos, et al., Application of the diffusion kurtosis model for the study of breast lesions, Eur. Radiol. 24 (2014) 1197–1203.
[21] D. Wu, G. Li, J. Zhang, et al., Characterization of breast tumors using diffusion kurtosis imaging, PLoS One 9 (2014) e113240.
[22] Breast Imaging Reporting and Data System, 5th ed., American College of Radiology, Reston (VA), 2013, pp. 1–25.
[23] E.R. DeLong, D.M. DeLong, D.L. Clarke-Pearson, Comparing the areas under two or more correlated receiver operating characteristic curves: a nonparametric approach, Biometrics 44 (1988) 837–845.
[24] G.M. Kacl, P. Liu, J.F. Debatin, et al., Detection of breast cancer with conventional mammography and contrast-enhanced MR imaging, Eur. Radiol. 8 (1998) 194–200.
[25] D. Le Bihan, Apparent diffusion coefficient and beyond: what diffusion MR imaging can tell us about tissue structure, Radiology 268 (2013) 318–322.
[26] A.B. Rosenkrantz, E.E. Sigmund, A. Winnick, et al., Assessment of hepatocellular carcinoma using apparent diffusion coefficient and diffusion kurtosis indices: preliminary experience in fresh liver explants, Magn. Reson. Imaging 30 (2012) 1534–1540.
[27] M. Iima, K. Yano, M. Kataoka, et al., Quantitative non-Gaussian diffusion and intravoxel incoherent motion magnetic resonance imaging: differentiation of malignant and benign breast lesions, Invest. Radiol. 50 (2015) 205–211.
[28] F. Grinberg, E. Farrher, L. Ciobanu, et al., Non-Gaussian diffusion imaging for enhanced contrast of brain tissue affected by ischemic stroke, PLoS One 9 (2014) e89225.
[29] H. Lu, J.H. Jensen, A. Ramani, et al., Three-dimensional characterization of non-Gaussian water diffusion in humans using diffusion kurtosis imging, NMR Biomed. 19 (2006) 236–247.
[30] C. Liu, K. Wang, X. Li, et al., Breast lesions characterization using whole-lesion histogram analysis with stretched-exponential diffusion model, J. Magn. Reson. Imaging: JMRI 47 (2017) 1701–1710.
[31] S. Suo, K. Zhang, M. Cao, et al., Characterization of breast masses as benign or malignant at 3.0T MRI with whole-lesion histogram analysis of apparent diffusion coefficient, J. Magn. Reson. Imaging: JMRI 43 (2016) 894–902.